International Review of Physics (I.R.E.PHY.), Vol. 5, N. 5
October 2011

Major Portions in Climate Change: Physical Approach

Jyrki Kauppinen, Jorma T. Heinonen, Pekka J. Malmi

Abstract – *The destroying of rainforests can warm the climate even more than the doubling of CO_2 concentration can do. The temperature close to the surface of the earth can change due to the change of the feedback or the amount of water in the atmosphere, without any forcing or change in the concentration of CO_2 as well as other greenhouse gases. This paper derives physically the sensitivity and the response time of the climate due to radiative forcing and a change in feedback. During the last century the temperature increase consisted of change in solar activity (0.47°C), destruction of rainforests (about 0.3°C), increase of the concentrations of the greenhouse gases (about 0.1°C) and increase of aerosols (about -0.06°C). About one half of the temperature increase was anthropogenic.*

Keywords: *Climate Change, Climate Sensitivity, Climate Response Time*

Nomenclature

T	Global mean temperature
T_e	Global mean temperature without greenhouse gases
ΔT_{2CO2}	Temperature increase due to doubling of CO_2
ΔT_Q	Temperature change due to radiative forcing
ΔT_G	Temperature change due to change of feedback
R	Climate sensitivity
R_0	Climate sensitivity without feedback
R_{av}	Average climate sensitivity
Q_s	Surface flux
Q	Absorbed flux
ΔQ	Radiative forcing
f	Feedback factor
F	Feedback loop gain
G	Feedback proportionality coefficient
p	Partial pressure of water vapor
C	Heat capacity
g	Step response
h	Impulse response
ϕ	Phase difference
τ	Response time
L	Diffusion length
D	Diffusivity

I. Introduction

The main goal of this paper is to calculate the change of the global mean temperature of the earth's climate due to a forcing like greenhouse gases and also without forcing. In addition, we like to know the corresponding response time. The temperature change ΔT_{2CO2} of the climate due to the doubling of the CO_2 concentration is still very uncertain.

According to the Intergovernmental Panel on Climate Change (IPCC) the change of the global mean temperature ΔT_{2CO2} is likely between 2 and 4.5 K, most likely 3.2 K [1]. Hansen et al. [2] have reported ΔT_{2CO2} between 2 and 5 K, assuming that the present temperature change results from the increased concentration of greenhouse gases. The major reason to the uncertainty is that the sensitivity R = dT/dQ of the climate is not very well known. The sensitivity gives us the surface temperature change $\Delta T = R\Delta Q$, where ΔQ (W/m^2) is the radiative forcing. Values of IPCC and Hansen imply that there is a positive feedback in the climate system. However, there are papers by Douglass et al. [3],[4] and Idso [5], where much smaller sensitivities are presented. These results are obtained e.g. from the annual solar irradiance cycle. Also Lindzen [6], Lindzen and Choi [7], Spencer and Braswell [8], [9] have reported a negative feedback.

The response times have been estimated from observed temperature profiles. The IPCC values are on the order of 10 -100 years, Meehl et al. [1] and Hansen et al. [2]. Using the autocorrelation study of the temperature curves, much smaller values like from 0.4 to 10 years are presented by Scafetta [10] and Schwartz [11]. The problem with these methods is that the response times of the climate and the forcing are mixed. Response times from 1 to 2 months are obtained by Douglass et al. [3],[4].

II. Estimation of Climate Sensitivity and Net Feedback

The total flux Q = 326 W/m^2 absorbed from the longwave emission is the incident surface flux Q_s = 396 W/m^2 minus the transmitted one 70 W/m^2, see Fig. 1 in [12]. The atmosphere absorbs a fraction ϵ =0.82 of the

Manuscript received and revised September 2011, accepted October 2011

surface radiation Q_s upwelling from the ground, or Q = ϵQ_s. The absorbed flux Q = 326 W/m^2 increases the temperature T close to the earth's surface by about 34 degrees, from 255 K to 289 K. Thus, the average sensitivity R_{av} is 34 K/(326 W/m^2) = 0.104 K/(W/m^2). Using linear approximation $\Delta T = R_{av}\Delta Q$, this gives for ΔT_{2CO2} only about 0.39 K, if the forcing ΔQ has the IPCC value 3.78 W/m^2. The above very rough estimation of the sensitivity gives us a hint to carry out a more detailed study based on the observed values of the climate.

We define the climate sensitivity R_0 without feedback as follows:

$$R_0(T) = \frac{dT}{dQ_s} = \frac{1}{4\sigma T^3} = \frac{T}{4Q_s} \tag{1}$$

where $Q_s = \sigma T^4$ is the blackbody emission flux from the earth's surface and σ is the Stefan Boltzmann constant. Integration gives the total forcing curve:

$$\Delta Q_s(T) = \sigma\left(T^4 - T_e{}^4\right) \tag{2}$$

where T_e is 255 K and the emissivity is set to unity. The total forcing in Q_s derived from the energy budget in [12] as the difference between the surface radiation 396 W/m^2 and the outgoing longwave radiation 239 W/m^2 is 157 W/m^2.

Notice that ΔQ_s(289 K), from equation (2), is about 156 W/m^2, which is close to the value derived from the energy budget. Taking into account all the possible feedback mechanisms we may write:

$$\begin{aligned} dT &= R_0(T)dQ_s = R_0(T)\left[dQ + f(T)dT\right] = \\ &= R(T)dQ \end{aligned} \tag{3}$$

where $R(T)$ is the actual sensitivity with all the feedback and $f(T)$ is a temperature dependent feedback factor. The forcing $dQ = d(\epsilon\, Q_s)$. From equation (3) we get:

$$R(T) = \frac{dT}{dQ} = \frac{R_0(T)}{1 - f(T)R_0(T)} = \frac{R_0(T)}{1 - F(T)} \tag{4}$$

or:

$$dQ = \left[\frac{1}{R_0(T)} - f(T)\right]dT \tag{5}$$

The integration of equation (5) should give the curve $Q(T)$, which starts at point A in Fig. 1(a), the condition without greenhouse gases, and goes through point B, the present condition of the climate.

We assume that the major feedback is proportional to the change of the water vapor concentration with temperature. Still simplifying, the feedback factor is assumed to be proportional to the derivative of the water vapor saturation pressure:

$$f(T) = -G\frac{dp}{dT} \tag{6}$$

where p is the saturation pressure of water vapor, and G is the proportionality coefficient.

We assume also that the surface albedo is constant. Integration of equation (5) gives:

$$\begin{aligned} Q(T) &= \int_{T_e}^{T}\left[\frac{1}{R_0(T)} + G\frac{dp}{dT}\right]dT = \\ &= \Delta Q_s(T) + G\left[p(T) - p(T_e)\right] \end{aligned} \tag{7}$$

As a first approximation, the water vapor saturation pressure is given by the Clausius-Clapeyron equation. We use here the Antoine equation, a simple empirical improvement to the Clausius-Clapeyron equation, widely used over limited temperature ranges [13]. The parameters for the range 273 - 473 K match fairly well with the experimental data down to T_e = 255 K. In the range under consideration the vapor pressure increases nearly exponentially with temperature, see Fig. 2.

Water vapor and clouds have a positive feedback in the longwave emission and a stronger negative feedback in incoming shortwave insolation. In addition, the latent heat gives more negative feedback. The slope of the curve $T(Q)$ in Fig. 1(a) represents the sensitivity of the climate. At point A the sensitivity R(255 K) without greenhouse gases is little less than R_0(255 K), which is 0.26 K/(W/m^2) according to equation (1). The reason is that even at the temperature 255 K we have a small derivative dp/dT and a weak feedback, which makes R(255 K) slightly smaller than R_0(255 K), according to equation (4). This is clearly seen in Fig. 1(b). So, the sensitivity at 255 K is substantially larger than R_{av} = 0.104 K/(W/m^2), the slope of the straight line between points A and B. We assume that the feedback does not change sign. This also means that the curvature of $T(Q)$ does not change sign. Hence, to go through points A and B the slope of $T(Q)$ at point B has to be substantially smaller than R_{av} and the net feedback has to be negative.

The sensitivity at B in Fig. 1(a) or at B' in Fig. 1(b) depends slightly on the shape of $T(Q)$. However, the shape determines how much smaller than 0.104 K/(W/m^2) the present sensitivity is.

For example, in Fig. 1(b) the sensitivity at B' is 0.058 K/(W/m^2) as calculated from equation (4) with $f = -Gdp/dT$, where G = 103 W/(m^{2}kPa). Another possibility to derive G is to use equation (7), where $G[p(T) - p(T_e)]$ should be (326 - 156) W/m^2 = 170 W/m^2.

It turns out that any monotonically decreasing function $f(T)$, which forces the curve $Q(T)$ to go through the points A and B so that the slope of $Q(T)$ at 255 K is very close to the slope of curve AC, has the derivative at point *B* between 0.05-0.07 K/(W/m²).

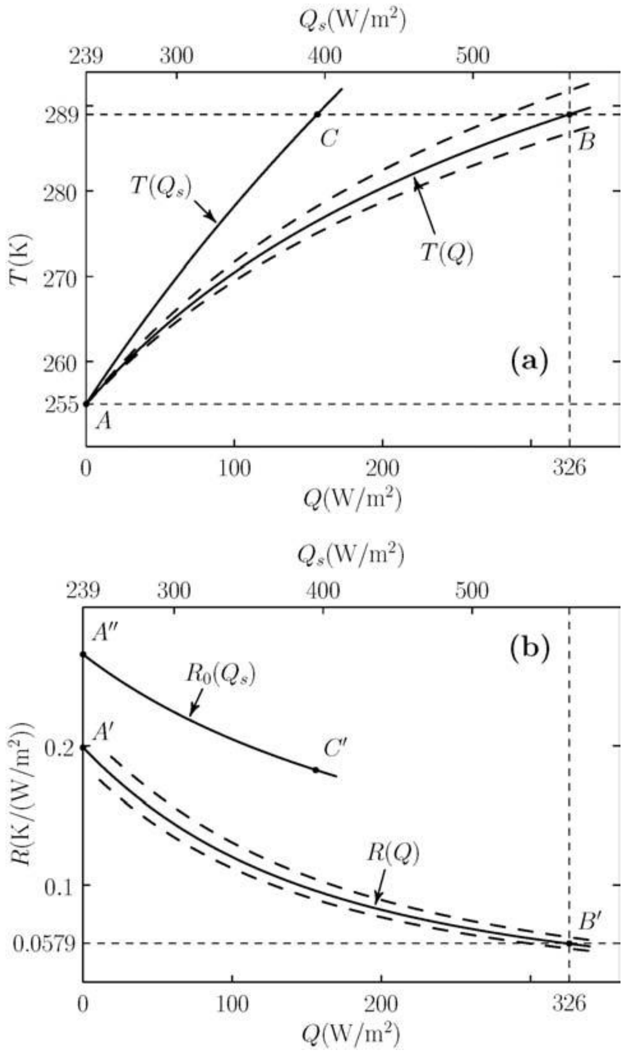

Figs. 1. (a) Temperature curves *AC*, $T(Q_s)$ without feedback and *AB*, $T(Q)$ with a net feedback. The points *A*, B and C are observed ones. The proportionality coefficient G in curve *AB* is 103 W/(m² kPa). The two extra curves are plotted with 25 % higher and lower *G*, for a purpose of comparison. (b) The corresponding sensitivities $R_0(Q_s)$ and $R(Q)$, the derivatives of $T(Q_s)$ and $T(Q)$, respectively

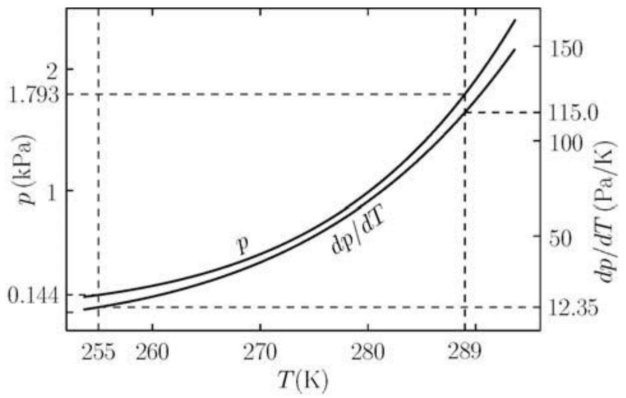

Fig. 2. The partial pressure of the saturated water vapor *p* and the derivative *dp/dT* as a function of temperature, according to Antoine equation

For example with 25 % larger or smaller *G* the derivatives are 0.054 K/(W/m²) and 0.063 K/(W/m²), respectively. See also point *B′* in Fig 1(b). This is very strong proof of the climate sensitivity.

Consequently the only possible choice for $f(T)$ is the amount of the water vapor and clouds in the atmosphere. In addition the speed of the hydrologic cycle has an effect on $f(T)$ via latent cooling.

In the real climate, both the forcing *Q* and the proportionality coefficient *G* can change. Then

$$\begin{aligned}\Delta T = & \ R\Delta Q - R\Delta G\left[p(T) - p(T_e)\right] = \\ & = \Delta T_Q + \Delta T_G\end{aligned} \tag{8}$$

where ΔT_Q and ΔT_G are the changes in temperature due to the changes of the forcing and the feedback, respectively.

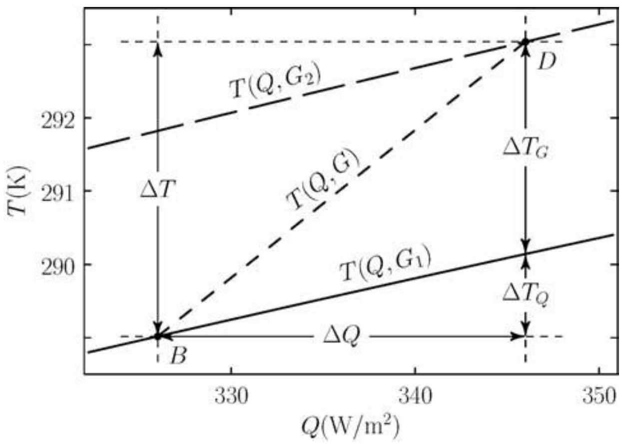

Fig. 3. The total temperature change is the sum of the contributions of the radiative forcing ΔQ and the change of the coefficient *G*. In the curves $T(Q, G_1)$ and $T(Q,G_2)$ the coefficient *G* is constant with $G_1 > G_2$. In the curve $T(Q,G)$ the coefficient *G* is changing. The point *B* is the same as the point *B* in Fig. 1(a)

The fictional situation, as demonstrated in Fig. 3, shows that the measured sensitivity $\Delta T/\Delta Q$, the slope of the curve $T(Q,G)$, can be much larger (or smaller) than the sensitivity due to the radiative forcing, the slope of the curve $T(Q,G_1)$ or $T(Q, G_2)$. So, the measured temperature curve as a function of the measured CO_2 concentration is not a very good tool for the estimation of ΔT_{2CO2} , because we cannot assume that ΔG is zero.

III. Physical Theory of the Response of the Climate

On the basis of our simplified estimation above, we conclude that we have to find a physical climate model i.e. the response of the climate, which gives the sensitivity and response time, as well. In physics, we describe any system by its impulse response $h(t)$, which contains all the information about the performance of the system in the domain *t*. Mostly *t* is time.

The output signal $S_{out}(t)$ is given by the convolution of the impulse response $h(t)$ and the input signal $S_{in}(t)$ as follows:

$$S_{out}(t) = h(t) * S_{in}(t) = \\ = \int_{-\infty}^{\infty} h(t') S_{in}(t-t') dt' \tag{9}$$

If the input signal is the Dirac delta function (unit impulse) $\delta(t)$, then the output signal is the impulse response of the system. On the other hand, if the input is a step function given by:

$$H(t) = \begin{cases} 1 & , \quad t \geq 0 \\ 0 & , \quad t < 0 \end{cases} \tag{10}$$

the output signal is a step response $g(t)$ of the system. The derivative of the step response gives the impulse response [14] i.e.:

$$h(t) = \frac{dg(t)}{dt} \tag{11}$$

First we define the climate system, which consists of the whole atmosphere including all the greenhouse gases, the surface of the earth to the depth of a few meters, all the lakes, and the mixing layer of the oceans to the depth of about 80 m. Later, we extend the thermodynamic climate system including the whole globe and atmosphere.

We assume that the climate is in a thermal equilibrium at the global annual mean temperature T_0 close to the surface. In addition, we have an energy balance on the surface and at the top of the climate. All types of energy circulation inside the system have a very small effect on the global mean temperature values, because the energy is moving in the atmosphere and in the oceans from one place to another so that the conservation of energy is valid.

More information is given in the discussion. Of course, these circulations have a great impact on the weather conditions. This theory deals with the global annual average values only. So, the temperatures can change locally, horizontally and vertically, for example, like the lapse rate in the atmosphere. The air temperature close to the earth's surface represents very well the temperature of the climate, because the major heat energy is close to the surface. The heat capacity of the air decreases exponentially with altitude. We calculate everything corresponding to an average vertical parcel of the climate system. The cross-section of the parcel is one square meter.

In order to find the impulse response of the climate system we derive first a step response. We assume that the climate at the equilibrium temperature T_0 senses an abrupt forcing ΔQ, which corresponds to the temperature increase of ΔT. The initial energy flux to the climate system is $\Delta Q = \Delta T/R$. With time the heating power per square meter is proportional to the difference between the final temperature $T_0 + \Delta T$ and the current temperature $T(t)$.

This process can be described by a simple differential equation:

$$C \frac{dT(t)}{dt} = \frac{T_0 + \Delta T - T(t)}{R} \tag{12}$$

where C is the total heat capacity of the climate system. If the sensitivity R is constant and the forcing starts at t =0, the solution of equation (12) is simply:

$$\frac{T(t) - T_0}{\Delta T} = 1 - e^{-t/\tau} \tag{13}$$

where $\tau = RC$ and $\Delta T = R\Delta Q$. Equation (13) gives us the step response, the derivative of which is the impulse response of the climate system:

$$h(t) = \frac{e^{-t/\tau}}{\tau} \tag{14}$$

The responses are shown in Figs. 4.

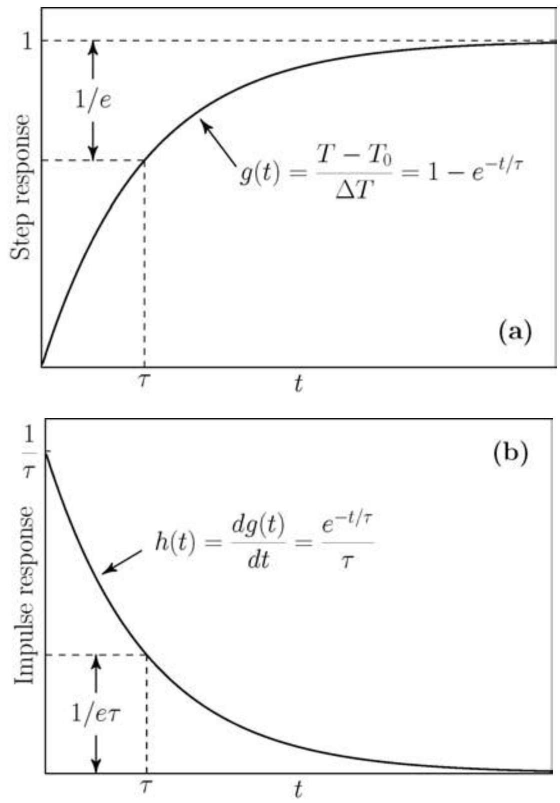

Figs. 4(a). The step response $g(t)$ and (b) the impulse response $h(t)$ of the climate system

IV. Derivation of the Sensitivity *R* and the Response Time *τ*

In climate research one possibility is to derive the climate parameters R and τ using glacial and recent temperature curves, i.e. $S_{out}(t)$ of the climate. Unfortunately, this is a very hopeless or even an impossible task, because we cannot derive $h(t)$ from $S_{out}(t)= h(t)*S_{in}(t)$. We will obtain only complicated information about both functions $h(t)$ and $S_{in}(t)$, and it is difficult to distinguish the impulse response $h(t)$. We have to know the forcing as a function of time, because $S_{in}(t)= R\Delta Q(t)$.

In addition, a change of the coefficient G can change the temperature without any radiative forcing. The other possibility is to use theoretical circulation models to derive the possible feedbacks and finally the sensitivity. See e.g. [2], [15]-[22].

Furthermore, in real climate it is almost impossible to arrange merely the step or unit impulse forcing. One possibility is to use a sinusoidal input. This is a common way to test electronic circuits. We have two options, namely the temperature profiles over day and night or over summer and winter. The diurnal temperature behavior may be too fast and it is not very sinusoidal. However, the annual temperature curve (not too close to the poles and the equator) seems to be close to sinusoidal. So, the forcing in the solar irradiation annual cycle is approximately:

$$S_{in}(t) = RA\cos\omega t \qquad (15)$$

where $\omega = 2\pi$/year and A is the amplitude of the solar forcing. Using equations (9), (14) and (15) we obtain:

$$\begin{aligned} S_{out}(t) &= RA\cos\omega t * h(t) = \\ &= RA_{out}\cos(\omega t - \phi) \end{aligned} \qquad (16)$$

where:

$$A_{out} = \frac{A}{\sqrt{1+(\omega\tau)^2}} = A\cos\phi \qquad (17)$$

is the amplitude of the temperature cycle and:

$$\phi = \tan^{-1}\omega\tau \qquad (18)$$

is the phase difference between the temperature and solar cycles. Finally, we obtain the response time:

$$\tau = RC = \frac{\tan\phi}{\omega} \qquad (19)$$

Because there is a nice analogy with an electronic RC-circuit, we can use it as a model as shown in Fig. 5.

The analogy between the climate system and electronic circuit parameters is as follows: voltage → temperature, electric current → heat current, electric capacitance → heat capacity, electric resistance → heat resistance, and electric charge → heat energy.

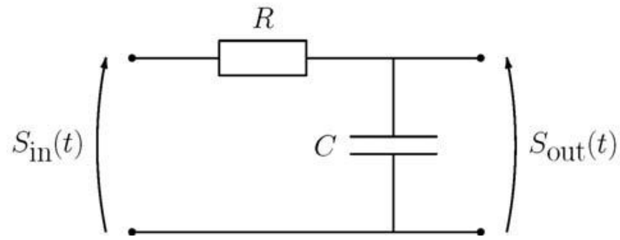

Fig. 5. *RC*-circuit model of the climate system

The basic idea is to measure ϕ and to calculate the heat capacity C of the climate, taking into account the heat capacity of the mixed layer in the ocean. The capacity over the ocean is larger than over the land. Thus, it is useful to apply the basic differential equation (12) separately to the land and to the ocean. After this we can calculate τ and R for land and for ocean using equation (19).

The heat capacity over land is the sum of heat capacities of air and a thin layer of the ground. The thickness of the layer is a fraction of the diffusion length. Our simulations later will give more information on the diffusion into the deep soil.

The heat diffusion lengths for the sinusoidal and for the step input are given by $L_{sin} = \sqrt{2D/\omega}$ and L_{step} $=1.264\ \sqrt{Dt}$, where D is the diffusivity of sandy soil, $2.4\cdot 10^{-7}$ m²/s [23].

According to the above equations the diffusion length for a step response is 2.24 times the diffusion length for a sinusoidal input with the same time scale. The heat capacity of the atmosphere is about 10.35 MJ/(Km^2) with a relative humidity of 70 %. The moisture of the soil increases the heat capacity.

The heat capacity over the ocean is a little different, because in the ocean there is a mixed layer with a thickness varying between 20 and 100 meters. The temperature of the mixed layer follows approximately the surface one.

This means that we have to take into account the heat capacity of the mixed layer. In addition, below the mixed layer we add the capacity of the layer, which is a part of the diffusion length like in the case of the soil. So, the total heat capacity over the ocean without the diffusion is about 325 MJ/(Km^2), which is the sum of the heat capacities of air and the mixed layer. The average thickness of the mixed layer is 75 m [24],[25]. The contribution of the diffusion to the heat capacity will be estimated in our simulations.

The thermal diffusivity of water is 1.410^{-7} m^2/s. The heat capacity over the ocean is about thirty times the heat capacity of the atmosphere.

V. Experimental Derivation of R and τ

We used the results of [26]. This paper is very helpful, because it gives the phase lags separately for the land and ocean. The mean lags between the annual temperature and solar irradiation cycles, observed from year 1954 to 2007, are 29±6 days over the land and 56±11 days over the ocean. We prefer using phase information instead of amplitude information, because the reference phase is exactly known at solstices. Thus, we need to know only the date of the annual temperature maxima or minima. Of course, it is possible to use the amplitudes A and A_{out} and to apply equation (17), but then we have to use two profiles, which both have measurement uncertainty.

The lags given by [26] correspond to the phase differences ϕ_{land} = 28.6° and ϕ_{ocean} = 55.2°. Substitution to equation (19) gives the response times τ_{land} = 1.04 months and τ_{ocean} =2.74 months, and the sensitivities R_{land} =0.244 and R_{ocean} =0.0222 K/(W/m^2). The rest of the results are collected in Table I.

The areas of land and ocean are roughly 29 % and 71 %, respectively. Because the temperature change over the land is one order of magnitude greater than that over the ocean, the global sensitivity depends substantially on how much the temperature changes balance out, e.g. by winds. We denote the extreme cases, which correspond to perfect imbalance and perfect balance by R_{glo1} and R_{glo2}, respectively. In the first case the global temperature change is simply the mean change weighted by the areas dT =0.29 dT_{land} +0.71 dT_{ocean}. Dividing by dQ we get:

$$R_{glo1} = 0.29R_{land} + 0.71R_{ocean} = 0.0863\frac{\text{K}}{\text{W/m}^2} \quad (20)$$

In the second case we assume that heat flows between land and ocean until the changes in temperature are equal. Conservation of energy requires that $0.29C_{land}dT_{land} + 0.71C_{ocean}dT_{ocean} = 0.29C_{land}dT + 0.71C_{ocean}dT$, where C_{land} and C_{ocean} are the heat capacities per unit area and dT is the common temperature change. Solving dT and dividing by dQ we get:

$$R_{glo2} = \frac{0.29C_{land}R_{land} + 0.71C_{ocean}R_{ocean}}{0.29C_{land} + 0.71C_{ocean}} = 0.0251\frac{\text{K}}{\text{W/m}^2} \quad (21)$$

The perfect balance is never reached globally but the local sensitivity on the coast should be close to R_{glo2}. According to [26], the lag on the coast is 42 days (ϕ = 41.4°). Substitution of this value to equation (19) gives τ_{coast} = 1.685 months.

The coast can be thought of as an area, which is half ocean and half land. If we use the average heat capacity C_{coast} =(C_{land}+C_{ocean})/2 = 168 MJ/K we get R_{coast} =0.026 K/(W/m^2). This value is in good agreement with the value R_{glo2}.

The final sensitivity is between R_{glo1} and R_{glo2} depending on how well the difference of the temperature change between the land and ocean is balanced. The linear combination 0.544R_{glo1} +0.456R_{glo2} is equal to the sensitivity 0.058 K/(W/m^2) derived in Fig. 1.

VI. Heat Diffusion Into the Thermocline and Into the Ground

The ocean consists of a mixed layer with an average thickness of 75 m. Below the mixed layer is the nearly permanent thermocline going down to 1000 m. In the average thermocline the temperature decreases from 16°C to 4°C. Below the thermocline is the deep ocean, where the temperature decreases very slowly a few degrees.

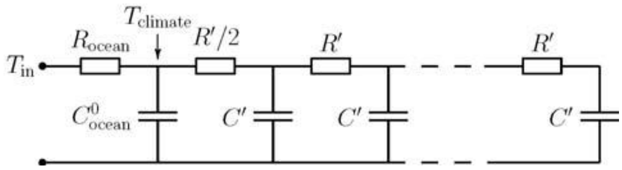

Fig. 6. $R'C'$-chain connected to the climate system

The diffusion into water in the ocean can be modeled by coupling an $R'C'$-chain parallel with the heat capacity of the mixed layer in the ocean C^0_{ocean} = 324.6 MJ/K as shown in Fig. 6. Now the heat capacity C^0_{ocean} does not include the diffusion layer below the mixed layer, so it is smaller than C_{ocean} (325.0 MJ/K) as demonstrated in simulations later. The diffusion takes place in the $R'C'$-chain. The heat resistance R' and the heat capacity C' of the water layer depend on the thickness of the layer. The heat resistance of one square meter parcel is 1.75 K/(W/m), and the heat capacity of the parcel is 4.19 MJ/(Km^3). The voltage at each junction of the $R'C'$-chain models the temperature of the corresponding layer. Figs. 7 show a simulation example of the ocean coupled with the diffusion layers. We used 48 layers with a thickness of 0.104 m, in other words 48 $R'C'$ circuits in the chain. The topmost curve in Fig. 7(a) is the step response of the coupled climate, and it is the temperature $T_{climate}$ (0 m) at the condenser C^0_{ocean} , when the temperature input step is one K. In addition, before the step input to the circuit all the 48 condensers of the $R'C'$-chain have been charged corresponding to the temperature profile of the thermocline. In the thermocline, just below the mixed layer, the temperature decreases about 0.03 K/m. Fig. 7(a) presents also the temperature profiles at a depth of 1 m, 2 m, and 5 m. Note that even at a depth of 5 m warming is quite slow. Using a sinusoidal input ΔT_{in} in the circuit of Fig. 6 with the angular frequency of 2π/year we can adjust R_{ocean} so that the phase angle is the observed one 55.2°. With this value of R_{ocean} we can calculate C_{ocean} using the relation $\tau_{ocean} = R_{ocean}C_{ocean}$. The difference C_{ocean}-C^0_{ocean} (very small = about 0.4 MJ/K) is the heat capacity of a part of the diffusion layer. This difference is greater (about 1 MJ/K) for the step input, because the thermal diffusion length is 2.24 times larger than in the case of a sinusoidal input. Fig. 7(b) demonstrates the diffusion to the thermocline with the sinusoidal input. The phase difference between the input and $T_{climate}$ (0 m) is 55.2°. Note that the amplitude of the signal obeys equation (17), even though we did not use this information. Part b presents also the temperatures at a depth of 1 m, 2 m, and 5 m from the bottom of the mixed layer. Similar treatment and simulations as above can be done for the climate over the land. In this case, the condensers in the *R′C′*-chain are charged at higher temperatures, because the temperature in the ground increases about 0.03 K/m. The heat diffusion into the soil has a greater effect on the sensitivity, because the capacity of the air (10.35 MJ/K) is much smaller than the capacity (324.6 MJ/K) in the case of the ocean. In the simulations we have used for the soil R' =3.33 K/Wm^2 and C' =1.28 MJ/Km. In the land case the capacities of the diffusion layer are approximately 0.4 MJ/K and 0.9 MJ/K for a sinusoidal and a step input, respectively.

Figs. 8 demonstrate a big difference between the continental and marine climates. Most people experience this effect very easily. Fig. 8(a) shows the step responses of the climate over the land, over the ocean, the step response of the global average climate without balancing the difference of the temperature change between the land and ocean (Glo1), and the step response with a 100 % Balanced climate (Glo2). In addition, Fig. 8(b) shows the final global step response and the step response on the coast. The global step response Global = 0.544 Glo1 + 0.456 Glo2, see Fig. 8(b). From this curve we are able to estimate the global response time 1.31 months. The step response on the coast should be very close to Glo2 because the mixing on the coast is close to 100 %. Using the *R′C′*-chain it is easy to calculate the slope of the step response at later times. The simulations show that the average climate warms about $3.5{\cdot}10^{-3}$ K between 10 and 20 years after the step of one K. This requires a forcing of 12 W/m^2 . The corresponding IPCC value is 0.1 K/10 years [1]. For the above results we have assumed that heat goes from the bottom of the mixed layer to the thermocline only by thermal diffusion. Of course, vertical convection increases heat conduction, as well. Using our simulation, we can easily calculate the case, where the conduction in the thermocline is hundreds of times the conductivity in heat diffusion in water.This corresponds to the Eddy diffusivity $1.4{\cdot}10^{-5}$ m^2/s [27],[28] in the ocean.

The results show that the sensitivity decreases 12 % and the temperature of the climate increases about $7.1{\cdot}10^{-3}$ K between ten and twenty years from the step of one degree. This step requires the forcing of 13 W/m^2 . Of course, with the forcing of 1.3 W/m^2 the temperature change of the climate is only $7.1{\cdot}10^{-4}$ K/10 years. Note that the IPCC value is 0.1 K/10 years.

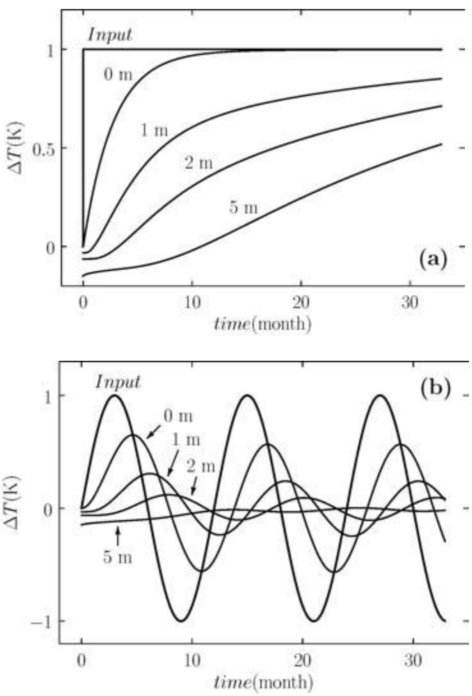

Figs. 7. (a). The step response of the climate coupled to the diffusion layer, and temperatures at different water layers Tclimate (0 m), 1 m, 2 m and 5 m below the mixed layer. b) The same demonstration using sinusoidal input with a year period. The phase difference between Input and Tclimate (0 m) is 55.2°

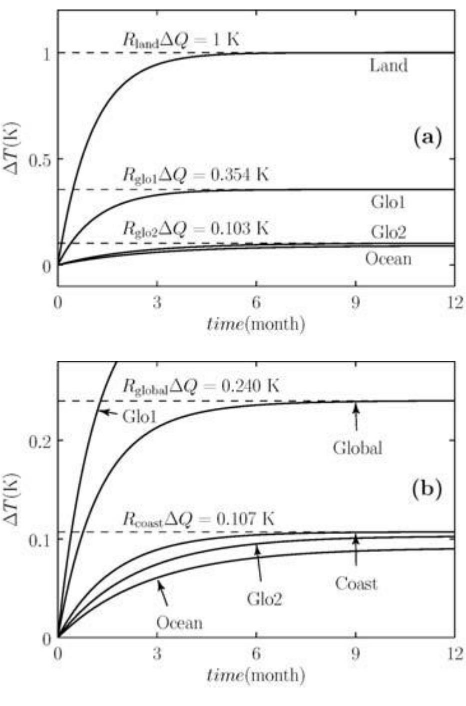

Figs. 8. All the step responses are drawn with the forcing of ΔQ = 1K/R_{land} =4.12 W/m^2 . (a) The step responses over the land and over the ocean. The step response Glo1 is the average weighted by the areas of land and ocean. The step response Glo2 is the average when the temperature difference between land and ocean is smoothed. (b)The extended part including the step response on the coast and the final global step response

VII. Application of the Model to CO_2

The doubling of CO_2 concentration gives a forcing of 3.78 W/m^2 (IPCC). In the literature, a smaller value of 2.4 W/m^2 can be found [29]. Using our average annual global sensitivity and the above forcings, we can calculate the change of the global mean temperature as follows

$$\Delta T_{2CO_2} = R_{global}\Delta Q = 0.058\cdot 3.78\text{K} = 0.22\text{K} \quad (22)$$

or:

$$\Delta T_{2CO_2} = 0.058\cdot 2.4\text{K} = 0.14\text{K} \quad (23)$$

These numbers are much smaller than IPCC values: 2 -4.5 K.

In this application we have to perform a small correction to the sensitivity. Our radiative forcing dQ includes also small positive feedbacks of water vapor and clouds in longwave absorptions. These are 1.4 W/(m^{2}K) and about zero, according to Fig. 3 in [19]. So, we have to use the forcing $\Delta Q_{2CO2}+\Delta Q_{water} \approx$ (3.78+1.4·0.22) W/m^2 = 4.09 W/m^2 . This gives $\Delta T_{2CO2} \approx$ 0.24 K. A better way to carry out this small correction is to add the water vapor feedback directly to the loop gain F , which changes to -2.13 +1.4R_0 = -1.88. thus, the sensitivity of the climate for all greenhouse gases, except water vapor, is R_g =0.063 K/(W/m^2).

Now the final values of ΔT_{2CO2} are 0.24 K and 0.15 K with the forcings 3.78 W/m^2 (IPCC) and 2.4 W/m^2, respectively. The results are in good agreement with the results by [30].

VIII. Effect of the Destruction of the Rainforests on the Global Mean Temperature

Fig. 1 shows also $T(Q)$-and $R(T)$-curves with 25 % smaller and larger coefficient G. These curves demonstrate that temperature can change much without any absorption forcing. Note that the sensitivity R changes very little. The temperature change is given by

$$\Delta T_G = -R\Delta G\left[p(T)-p(T_e)\right] \quad (24)$$

Approximately a 10 % change in G corresponds to the temperature change of 1 K. A good example of this is a change in the solar activity, which changes the cloudiness of the atmosphere. The clouds have a strong negative feedback. This has a much bigger effect on the temperature than a small radiative forcing (about one per mil) due to the change of the insolation [31]. Also aerosols can change G.

One more important example about the use of the equation (24) is the estimation of the temperature change due to the destruction of the rainforests. The feedback loop gains:

$$F = f(T)R_0 = -G\frac{dp(T)}{dT}R_0 \quad (25)$$

derived for land, for ocean and for globe are 0.25, -7.28, and -2.13, respectively, see Table I.

Then the corresponding coefficients G are roughly:
G_{land} = -12 W/(m^{2}kPa) ,
G_{ocean} = 348 W/(m^{2}kPa) and
G_{global} = 103 W/(m^{2}kPa).

These values are global mean ones at the average temperature 289 K. In rainforests vaporization is very effective, because the evaporation is abundant due to the stratification of large-area leaves in the vegetation. The relative humidity is high and also cloudiness is high due to thunderstorms. The hydrologic cycle is very rapid. Thus we can assume that $G_{rainforest} \geq G_{ocean}$. If man destroys the rainforest over an area of A_0 and after the destruction the area is like average land with G_{land} = -12 W/(m^{2}kPa), then the total change of G is G_{ocean} -G_{land} = 360 W/(m^{2}kPa) or larger. This corresponds to the change of about:

$$\Delta G_{global} = -\frac{A_0}{A}360\frac{\text{W}}{\text{m}^2\text{kPa}} \quad (26)$$

where A is the area of the earth globe. For example if A_0/A =1 % or $A_0 \approx 5.4\cdot 10^6$ km^2, the global mean temperature change according to equation (24) is about 0.3 K. So, it is much easier for us to cause a bigger climate change by destroying rainforests than by increasing CO_2 concentration in the atmosphere.

The above example corresponds to the case, where 1 % of the area of the earth is changed from ocean to land.

TABLE I
CLIMATE RESPONSE TIMES T, SENSITIVITIES R, HEAT CAPACITIES C AND FEEDBACK LOOP GAINS F

	τ (month)	R(K/(W/m^2))		C(MJ/(Km^2))		F
		sinusoidal	step	sinusoidal	step	
Land	1.04	0.254	0.243	10.8	11.2	+0.25
Ocean	2.74	0.0222	0.0221	325	326	-7.28
Glo1	1.15	0.0893	0.0863			-1.12
Glo2	2.35		0.025			-6.32
Coast	1.69		0.026		168	-6.04
Global (Fig. 1)			0.058			-2.13
Global	1.31		0.058			-2.13

If we replace the relative areas of 29 % and 71 % with 30 % and 70 % for land and ocean, respectively, equations (20) and (21) give a new global sensitivity R_{global} =0.0596 K/(Wm^2). This means that the feedback loop gain *F* is changed from -2.13 to -2.05 giving the change of *G* about -4 W/(m^{2}kPa). This result supports the value -3.6 W/(m^{2}kPa), given in equation (26). Quite large areas of the rainforests have been destroyed since 1970 [32]. This explains at least partly the rapid temperature increase in the same time period.

IX. Discussion

Finally, we like to point out that according to our results there is no so called faint young sun paradox [33]. Assuming that during the faint young sun the insolation was 25 % smaller than now the temperature change was about 0.058 K/(W/m^2)(-0.25·341W/m^2) ≈ -5K. So the temperature was only 5 K lower than now and our globe was not frozen. In addition, the coefficient *G* was smaller than 103 W/(m^{2}kPa), because the amount of biomass was smaller than now.

In this paper we have assumed that the surface albedo and the coefficient *G* are constants all the way from *A* to *B* in Fig. 1(a). It turns out that the change of the surface albedo would make the curve *AB* to start with a little higher and end with a little lower slope. In our model this means that the coefficient *G* would change from a little lower to a little higher value than 103 W/(m^{2}kPa) on the way from *A* to *B*. Solar energy is also stored in mechanical forms like wind, waves and streams in the oceans, and potential energy. These energies are very small compared with the thermal energy stored in the climate and ocean. Usually these mechanical energies increase when the temperature of the climate increases, so they increase the negative feedback slightly. We have to point out that the sensitivity and response times can change slowly, for example, due to the changes of the surface albedo and the temperature. As shown in Figs. 1, the sensitivity of the climate decreases, when the temperature and forcing increase. This corresponds to the extra negative feedback in the climate.

In the climate, the heat energy circulation does not change the average temperature, if the circulation takes place along a path, where the heat capacity is constant. For example, wind over the ocean or a stream in the ocean has a minor effect on the average global temperature. However, if the wind is crossing the coast, the average temperature can change, because the heat capacity over the ocean is thirty times of that over the land. This is the greatest effect on the average temperature, due to circulation.

X. Conclusion

We have estimated the global mean sensitivity of the climate using two independent physical methods. The simplified method uses three well-known points (*Q*, T), the points *A*, *B* and *C* in Fig. 1(a), and a single adjustable parameter *G*. The other method uses two experimental phase lags between the annual solar irradiation cycle and the annual temperature curve, one for the ocean and one for the land. Since the annual solar irradiation cycle is well known the response time of the climate is only a function of the phase lag. In this method we need to know only the shapes of the irradiation and temperature curves, the absolute amplitudes are not relevant. So, the long-term variation of forcings and feedback has a minor effect on these results. We apply only the conservation of energy to the climate system as a function of time. The basic physics is in the differential equation (12).

Our values for the sensitivity and response time are in good agreement with each other and much smaller than the values reported earlier by studies based on the experimental temperature curves. We should realize that the temperature curve is a result of the solar activity and other forcings as well as the feedback. It is practically impossible to separate the roles of these factors in climate change merely from the temperature curve.

We believe that the greatest changes in temperature are due to the change in the proportionality coefficient *G*, i.e. the relation between cloudiness and water vapor concentration. The temperature increase of the last century can be explained almost completely by the increase of solar activity and the decrease of cosmic ray flux together 0.47 K [31], the destruction of rainforests about 0.3 K, the increase of greenhouse gas concentration about 0.1 K and increase of aerosol about -0.06 K [1]. The sum of these contributions is 0.81 K, which is close to the observed temperature increase [34].

In the end, we conclude that maybe one reason for the long history of life on our globe is the negative feedback of the climate for the global temperature.

References

[1] G. A. Meehl, T. F. Stocker, W. D. Collins, P. Friedlingstein, A. T. Gaye, J. M. Gregory, A. Kitoh, R. Knutti, J. M. Murphy, A. Noda, S. C. B. Raper, I. G. Watterson, A. J. Weaver, and Z.-C. Zhao. Global climate projections. contribution of working group i to the fourth assessment report of the intergovernmental panel on climate change. In S. Solomon, D. Qin, M. Manning, Z. Chen, M. Marquis, K.B. Averyt, Tignor M., and H.L. Miller, editors, *Climate Change 2007: The Physical Science Basis. Contribution of Working Group I to the Fourth Assessment Report of the Intergovernmental Panel on Climate Change*, IPCC Assesment Reports, chapter 10. Cambridge University Press, 2007.

[2] J. Hansen, A. Lacis, D. Rind, G. Russel, P. Stone, I. Fung, R. Ruedy, and J. Lerner. Climate sensitivity: Analysis of feedback mechanisms. *Climate Processes and Climate Sensitivity*, 5:130–163, 1984.

[3] D. H. Douglass, E. G. Blackman, and R. S. Knox. *Physics Letters A*, 323:315–322, 2004.

[4] D. H. Douglass, E. G. Blackman, and R. S. Knox. *Physics Letters A*, 325:175–176, 2004.

[5] Sherwood B. Idso. CO_2-induced global warming: a skeptic's view of potential climate change. *Climate Research*, 10:69–82, 1998.

[6] R. S. Lindzen. Taking greenhouse warming seriously. *Energy & Environment*, 18:937–950, 2007.

[7] R. S. Lindzen and Y-S. Choi. On the determination of climate feedbacks from erbe data. *Geophysical Research Letters*, 36,

2009.

[8] R. W. Spencer and W. D. Braswell. Potential biases in feedback diagnosis from observational data: A simple model demonstration. *Journal of Climate*, 21:5624–5628, 2008.

[9] R. W. Spencer and W. D. Braswell. On the diagnosis of radiative feedback in the presence of unknown radiative forcing. *Journal of Geophysical Research*, 115(D16109), 2010.

[10] N. Scafetta. Empirical analysis of the solar contribution to global mean air surface temperature change. *Journal of Atmospheric and Solar-Terrestrial Physics*, 71:1916–1923, 2009.

[11] S. E. Schwartz. Heat capacity, time constant, and sensitivity of earths climate system. *Journal of Geophysical Research*, 112(D24S05), 2007.

[12] K. E. Trenberth, J. T. Fasullo, and J. Kiehl. Earth's global energy budget. *Bulletin of the American Meteorological Society*, 90:311–324, 2009.

[13] B. E. Poling, J. M. Prausnitz, and J. P. O'Connel. *The Properties of Gases and Liquids*. McGraw-Hill, New York, 2000.

[14] J. Kauppinen and J. Partanen. *Fourier Transforms in Spectroscopy*. Wiley-VHC, Berlin, 2001.

[15] J. Hansen, A. Lacis, R. Ruedy, M. Sato, and H. Wilson. How sensitive is the world's climate? *National Geographic Research & Exploration*, 9:142–158, 1993.

[16] J. Hansen, G. Russel, A. Lacis, I. Fung, and D. Rind. Climate response times: Dependence on climate sensitivity and ocean mixing. *Science*, 229:857–859, 1985.

[17] B. J. Soden and I. M. Held. An assessment of climate feedbacks in coupled ocean-atmosphere models. *Journal of Climate*, 19:3354–3360, 2006.

[18] S. Bony, R. Colman, V. M. Kattsov, R. P. Allan, C. S. Bretherton, J-L. Dufresne, A. Hall, S. Hallegatte, M. H. Holland, W. Ingram, D. A. Randall, B. J. Soden, G. Tselioudis, and M. J. Webb. How well do we understand and evaluate climate change feedback processes? *Journal of Climate*, 19:3445–3482, 2006.

[19] R. Colman. A comparison of climate feedbacks in general circulation models. *Climate Dynamics*, 20:865–873, 2003.

[20] J. T. Kiehl. Atmospheric general circulation modeling. In K. E. Trenberth, editor, *Climate System Modeling*, chapter 10. Cambridge University Press, New York, 1992.

[21] J. M. Gregory, R. J. Stouffer, S. C. B. Raper, P. A. Stott, and N. A. Rayner. An observationally based estimate of the climate sensitivity. *Journal of Climate*, 15:3117–3121, 2002.

[22] P. M. D. Forster and J. M. Gregory. The climate sensitivity and its components diagnosed from earth radiation budget data. *Journal of Climate*, 19:39–52, 2006.

[23] S. P. Arya. *Introduction to Micrometeorology*, volume 79 of *International Geophysics*. Academic Press, London, second edition, 2001.

[24] R. Goody. *Principles of Atmospheric Physics and Chemistry*. Oxford University Press, New York, 1995.

[25] D. L. Hartmann. *Global Physical Climatology*, volume 56 of *International Geophysical Series*. Academic Press, San Diego, 1994.

[26] A. R. Stine, P. Huybers, and I. Y. Fung. Changes in the phase of the annual cycle of surface temperature. *Nature*, 457:435–440, 2009.

[27] H. E. Sweers.Vertical diffusivity coefficient in a thermocline. *Limnology and Oceanography*, 15:273–280, 1970.

[28] R. H. Stewart. Introduction to physical oceanography, 2007. Section 8.5, Mixing in the Ocean.

[29] A. Zastawny.Calculation of solar and thermal radiation absorption in the atmosphere, based on the hitran data. *Meteorology and atmospheric physics*, 92:153–159, 2006.

[30] F. M. Miskolczi. Geenhouse effect in semi-transparent planetary atmospheres. *Időjárás*, 111:1–40, 2007.

[31] N. J. Shaviv. On climate response to changes in the cosmic ray flux and radiative budget. *Journal of Geophysical Research*, 110:1–15, 2005.

[32] J. Parantainen. Tuuletusta ilmastokeskusteluun: konvektio ja sademetsien hupenevat ukkospilvet. *Tieteessä tapahtuu*, 25, 2007.

[33] D. Rind. The sun's role in climate variations. *Science*, 296:673–677, 2002.

[34] B. Liebmann, R. M. Dole, C. Jones, I. Blad, and D. Allured. Influence of choice of time period on global surface temperature trend estimates. *American Meteorological Society*, pages 1485–1491, 2010.

Authors' information

[1] Department of Physics and Astronomy University of Turku FI-20014 TURKU, FINLAND.
E-mail: jyrki.kauppinen@utu.fi

Jyrki K. Kauppinen was born in Finland in 1944. He was received his Bachelor of Arts degree in 1967, his M.Sc.degree in Physics in 1968, and the Ph.D. degree in 1975 from the University of Oulu. He started his academic career at the University of Oulu working in many positions from assistant to professor. The National Research Council of Canada appointed him a research fellow in 1980. Dr. Kauppinen was elected as senior research fellow at the Academy of Finland in 1981. He has also worked at the Technical Research Center of Finland and the Metrology Research Institute of Helsinki University of Technology. In 1990 he was a visiting scientist at the National Research Council of Canada and at Kansas State University. At present he is a professor of Physics at the University of Turku (since 1986), a docent in Physics at the University of Oulu, and a docent in Optical Measurement Technology at Aalto University in Espoo.

Professor Kauppinen has published about 160 papers in international scientific journals and has made about 140 conference presentations including about 50 invited lectures. He has written invited review-articles in Encyclopedia of Applied Physics, in Encyclopedia of Spectroscopy and Spectrometry, in Spectrometric Techniques, in Optics Encyclopedia, and in Handbook of Vibrational Spectroscopy. His paper dealing with Fourier Self-Deconvolution has the highest citation number in the whole history of the Journal of Applied Spectroscopy. In 2001 Kauppinen and Partanen published a book Fourier Transforms in Spectroscopy (Wiley-VCH). He has 22 patents or patents pending.

He has been for example a member of the program and steering committees in the International Conferences on Fourier Transform Spectroscopy, a member of the working group of IUPAC for Unified Wavenumber Standards, a member of Finnish Academy of Science and Letters, and a member of the editorial board of Applied Spectroscopy Reviews. He was the chairman of the program committee and a member of the steering committee for the first International Conference of Advance Vibrational Spectroscopy ICAVS-1 held in Turku. He was also a member of the program and steering committees for ICAVS-2.

He has received the International Bomem-Michelson Award in 1992 and the Innovation Award (the Foundation for New Technology) in 1999 and in 2005 for developing the commercial FTIR gas analyzer GASMET with Temet Instruments Ltd.

His varied research interests include high-resolution Fourier transform spectroscopy, development of high-resolution interferometers. He built his first high resolution FTIR spectrometer at the University of Oulu. This spectrometer was the fifth high resolution FTIR instrument in the world starting to record spectra in 1971. All the time the resolution of the spectrometer has been the highest one in the world. Later Dr. Kauppinen modified the interferometer using the first time home made cube-corner mirrors. The modified cube-corner interferometer achieved the resolution of 0.001 cm^{-1}, which is still the highest practical resolution. At the University of Turku he has built a new cube-corner interferometer with a resolution of 0.0004 cm^{-1}. Further, he has produced infrared wavenumber standards and studied a lot of rotation-vibration spectra of molecules including all the greenhouse gases with his high resolution interferometer. He has developed the gauge measuring interferometer for the Finnish standard of length, low-resolution stationary interferometers (without moving parts), small very stable low resolution interferometers for IR, NIR, VIS, and UV such as Carousel-interferometer, Pendium interferometer, and Diamond interferometer, an automatic, commercial, portable FTIR gas analyser GASMET. Dr. Kauppinen has developed data processing by various

sophistic mathematical methods such as resolution enhancement using Fourier Self-Deconvolution and the extrapolation of signals. Two spin-off companies have been founded based on his research work.
His latest innovation was an optical microphone using silicon cantilevers. This microphone has been used in photoacoustic spectroscopy to improve sensitivity. There are a few commercial instruments based on his microphone. In principle, photoacoustic detection of gases is based on the greenhouse phenomenon in a small gas chamber.

Jorma T. Heinonen received his M.Sc. degree from University of Turku, Finland, in 1974 and his Licenciate in Philosophy degree in 1980 from the same university. He works as a Laboratory Manager in the Department of Physics and Astronomy. His research interests have been in exploitation of solar energy and simulation and development of the photoacoustic cell.

Pekka J. Malmi received his M.Sc degree from the University of Turku, Finland, in 1990 and his Ph.D. degree in 1999 from the same university. He works as an University Lecturer in the Department of Physics and Astronomy. His research interests have been in low temperature solid state NMR and ESR, especially in quantum crystals. His current interests are in the field of optical spectroscopy.